Palaeogeography, Palaeoclimatology, Palaeoecology 415 (2014) 225–232

Contents lists available at ScienceDirect

Palaeogeography, Palaeoclimatology, Palaeoecology

journal homepage: www.elsevier.com/locate/palaeo

Reconstruction of southwestern Atlantic sea surface temperatures during the last Century: Cabo Frio continental shelf (Brazil)

L.G.M.S. Cordeiro [a], A.L. Belem [a], I. Bouloubassi [b], B. Rangel [a], A. Sifeddine [a,b,c], R. Capilla [d], A.L.S. Albuquerque [a,*]

[a] Geochemistry Department, Universidade Federal Fluminense, Niterói, RJ, Brazil
[b] LOCEAN-IPSL (CNRS/IRD/UPMC/MNHN), Paris, France
[c] LMI PALEOTRACES (IRD/UFF/Uantof), Geochemistry Department, UFF, Niterói, RJ, Brazil
[d] CENPES-PETROBRAS, Rio de Janeiro, RJ, Brazil

ARTICLE INFO

Article history:
Received 9 July 2013
Received in revised form 18 January 2014
Accepted 22 January 2014
Available online 31 January 2014

Keywords:
$U^{K'}_{37}$-SST
SW Atlantic
Cabo Frio
Western boundary upwelling system

ABSTRACT

Modern sea surface temperatures (SSTs) were estimated from $U^{K'}_{37}$ values of ten core-top sediment samples collected under the Cabo Frio upwelling system and validated by comparison with satellite-derived SSTs. $U^{K'}_{37}$-SSTs were found to reflect annual SST means in the offshore area and seasonal means (winter/spring) in the inshore and central areas. The latter areas are mainly influenced by upwelling processes whereas the offshore area is under the influence of the thermal front of the Brazil Current (BC). SST variability during the last century was then reconstructed from three short sediment cores. The record showed a general cooling trend in the inshore and central areas, suggesting intensification of the upwelling process. The trends at the offshore area reflected oscillations of the BC thermal front, with piling up of warmer BC waters closer to the coast since ca. 1950.

1. Introduction

The reconstruction of past sea surface temperatures (SSTs) from marine archives is crucial to improve our understanding of ocean variability and how much of it is due to ocean–atmosphere interactions or internal dynamics, a key issue of climate research.

Alkenone-$U^{K'}_{37}$ is well established as a robust and reliable proxy for reconstruction of past SST (see reviews by Herbert, 2003; Sachs et al., 2007). A number of factors that potentially could influence the $U^{K'}_{37}$ index (e.g. light/nutrient levels, diagenesis) have been shown to little affect the reliability of $U^{K'}_{37}$-SST reconstructions. However, there are still two main issues to consider. Although most studies assume that $U^{K'}_{37}$ values reflect temperatures at the sea surface, the depth of maximum production can show regional differences. In addition, alkenone production from coccolithophorids generally shows strong seasonality that may, in some cases, result in sedimentary $U^{K'}_{37}$ values reflecting seasonal instead of mean annual temperatures (Leduc et al., 2010a). It was recently shown that the seasonality of the maximum alkenone flux in sediment traps varies markedly across the oceans, depending not only on latitude and light availability but also on local oceanographic conditions (Rosell-Melé and Prahl, 2013). In addition, advection of the fine-particles that are the alkenone carriers may additionally challenge interpretations of the proxy, as evidenced in the Malvinas Current region (Benthien and Müller, 2000). Therefore, there is a need to constrain the application of the $U^{K'}_{37}$-SST proxy in different environments through investigations on modern and/or recent past settings and comparisons with instrumental data.

Documenting the South Atlantic SST variability is of great interest given its role in the global distribution of heat, which, in turn, governs climate. Seasonal and interannual variability of South Atlantic SST plays a fundamental role in the dynamics of the South Atlantic Convergence Zone (SACZ) (Robertson and Mechoso, 2000; Liebmann and Marengo, 2001; Chaves and Nobre, 2004), which represents one of the main features of the South American Monsoon System (SMAS) (Zhou and Lau, 1998; Carvalho et al., 2004) that controls summer precipitation over the southwestern portion of the continent. There are some sediment SST records in the South Atlantic, several in the eastern part (Müller et al., 1998; Kim et al., 2002, 2003; Sachs and Anderson, 2003; Kim et al., 2008; Leduc et al., 2010a) and fewer in the western one (Benthien and Müller, 2000; Jaeschke et al., 2007; Kim et al., 2008; Leduc et al., 2010b). But these studies mostly deal with deep ocean settings for rather large time windows. SST records for coastal sites and/or focused on the recent past, thus enabling comparisons with available instrumental data, are insufficient, with only one done by Mahiques et al. (2005) for the South-Eastern Brazilian Continental Margin (SEBCM).

The Cabo Frio Upwelling System (CFUS) in the SW Atlantic is particularly interesting because it is a western boundary upwelling system. It is located in an area where there is a conspicuous change in the shoreline orientation and where synergetic oceanographic mechanisms result in different upwelling areas on the shelf (Belem et al., 2013). Productivity and sedimentation patterns promote organic matter

* Corresponding author at: Programa de Geoquímica Ambiental, Departamento de Geoquímica, Universidade Federal Fluminense, Outeiro São João Baptista s/n, Niterói, RJ CEP 240120-015, Brazil. Tel.: +55 21 2629 2197.
E-mail address: ana_albuquerque@id.uff.br (A.L.S. Albuquerque).

0031-0182/$ – see front matter © 2014 Elsevier B.V. All rights reserved.
http://dx.doi.org/10.1016/j.palaeo.2014.01.020

accumulation areas, especially on a mud bank situated roughly along the 100 m isobath in front of Cabo Frio, with a north-southeast direction. Such areas are of particular interest because they allow for proxy reconstructions at high time resolution.

In order to document (multi)decadal SST oscillations for the last century, possibly linked to the upwelling variability, we reconstructed $U^{K'}_{37}$-SST from three short sediment cores recovered along a cross-shelf transect on the mud bank of the Cabo Frio continental shelf. To further constrain the use of the $U^{K'}_{37}$-SST proxy we also studied ten core-tops and compared reconstructed SST with instrumental-derived data (SeaWiFS, AVHRR and ICOADS/ERSST).

2. Materials and methods

2.1. Regional setting

The regional oceanography of CFUS is characterized by three main water masses: the surface warm and low salinity Coastal Water (CW), which flows over the inner shelf (>15 °C, salinity of 32–34 psu, <30 m depth) and results from the dilution of oceanic waters with continental drainage water; the surface warm and saline Tropical Water (TW), flowing offshore (24–28 °C, salinity of ~37 psu, 0–200 m depth), which comprises the southward branch of the Brazil Current (BC), the main current in the area; and the South-Atlantic Central Water (SACW: <18 °C, salinity of 35–36.4 psu), which is almost constantly located at the shelf bottom (>110 m depth). The complex interactions of these water masses are thought to control the sedimentation processes on the SEBCM (Mahiques et al., 2004).

Previous studies linked the occurrence of upwelling to the sudden change in the axis of the continental shelf, followed by the north–south oriented Brazil Current (BC) (Rodrigues and Lorenzzetti, 2001). This setting results in an intermittent surface upwelling of cold and nutrient-rich SACW at a focal point close to Cabo Frio Island or in a subsurface upwelling at mid-shelf (Valentin et al., 1987; Aidar et al., 1993; Franchito et al., 2008). Moreover, the typical coastal upwelling mechanism takes place on the inner shelf (0 to ~10 km from coast), largely induced by northeasterly trade winds that favor the Ekman offshore transport of surface waters (CW and TW) and result in the intrusion of SACW over the shelf and into surface waters (Moreira da Silva, 1973; Valentin and Kempf, 1977; Valentin, 1984; Castelao and Barth, 2006; Franchito et al., 2008). However, the CFUS system appears to be more complex than previously thought. On the mid-shelf the interaction of the wind curl, thermal fronts and eddies induced by the meandering of the BC can favor the upwelling of SACW into the euphotic zone (Castro and Miranda, 1998; Castelao and Barth, 2006; Silveira et al., 2008). At the shelf break, regional dynamics related to the BC thermal front positioning have also been shown to favor the intrusion of SACW into the euphotic zone (Belem et al., 2013), contrasting with the major influence of warmer waters from BC in this region.

The upwelling at Cabo Frio is intermittent, occurring as short episodic events all year-round, but particularly enhanced during austral spring/summer under prevailing NE winds on the inner shelf (Castro et al., 1987; Campos et al., 2000). In contrast, cold front S-SW winds during fall and winter inhibit the surface upwelling of SACW (Valentin et al., 1987). On the mid- and outer shelf, Ekman pumping induced by negative wind stress curl not only occurs year-round but also reaches maximum values in summer (Castelao and Barth, 2006).

The upwelling at Cabo Frio induces pulses of enhanced chlorophyll concentrations (0.5 to 6.0 mg Chl-a m^{-3}) in the area close to the coast (Valentin and Coutinho, 1990; Gonzalez-Rodriguez et al., 1992). Although these levels are much lower than those observed in eastern boundary upwelling regions, such as Benguela: 15–31 mg Chl-a m^{-3} (Estrada, 1980) and Peru: 10–40 mg Chl-a m^{-3} (Strickland et al., 1969), they contrast with the overall oligotrophic conditions in continental shelf and open waters off the Brazilian coast that are dominated by warm tropical waters (Marone et al., 2010). Most importantly, the elevated phytoplanktonic production of the Cabo Frio upwelling sustains one of the most important fishery areas of the Brazilian continental shelf (Moreira da Silva, 1971). Upwelling plumes also contribute in the fertilization of adjacent areas and the export of biomass, which results in organic-enriched deposits along the transport pathway (Lorenzzetti and Gaeta, 1996).

A unique sedimentological feature along the continental shelf is a fine-grained deposit southeast of Cabo Frio Island, extending roughly over the 100 m isobath in a north-southeast direction. This "mud bank" was first mapped by Dias et al. (1982) and subsequently by Mahiques et al. (2004). There, sediments are characterized by high contents of silt–clays, especially in its central area (Cruz et al., 2013; Sanders et al., 2014), relatively elevated total organic carbon (TOC) and the presence of fresh organic matter (Mahiques et al., 2004, 2005; Yoshinaga et al., 2008; Sanders et al., 2014). Sediment cores in this area likely have a high potential for recording past biogeochemical and oceanic variability at elevated time resolution.

2.2. Sampling location

Three box cores (ca. length of 20 cm, BCCF10-15, BCCF10-09, BCCF10-01) and ten core-top samples (CT, first 0.5 cm) were retrieved in April 2010 along the mud bank on the continental shelf of Cabo Frio. The sampling stations were located within an area of ca. 600 km^2 (10–60 km offshore; 80–130 m water depth) (Fig. 1 and Table 1). The box cores used for SST reconstruction were sampled continuously at 1-cm sampling steps.

2.3. Alkenone analysis and $U^{K'}_{37}$-SST estimation

Alkenones were extracted from dried sediments (ca. 4 g) with a mixture of dichloromethane/methanol (3/1, v/v) in an ultra-sonic bath and isolated via silica-gel chromatography using solvent mixtures of increasing polarity. They were analyzed by gas chromatography on an Agilent 6890Plus series gas chromatograph equipped with a DB-5MS fused silica capillary column (60 m, 0.32 mm i.d., 0.25 μm film thickness). Helium was used as the carrier gas. The GC oven temperature was programmed to increase from 50 °C to 140 °C at 30 °C min^{-1} (3 min hold time), then to 280 °C at 20 °C min^{-1} and to 310 °C at 0.5 °C min^{-1}. The temperature of the on-column injector was programmed at the oven track mode, and the Flame Ionization Detector (FID) was set to 320 °C. A known amount of $C_{36}H_{74}$ was added to the alkenone fraction prior to GC injection for quantitation. Selected samples were analyzed by gas chromatography–mass spectrometry (GC–MS) to confirm the alkenone identification and the absence of coeluting compounds. GC–MS analyses were carried out on an Agilent 6890N GC coupled to an Agilent 5973N MSD, operated with ionization energy of 70 eV and a scanning mass range of m/z 50–800 at 3 scans per second.

SSTs were estimated from the alkenone $U^{K'}_{37}$ index $((C_{37:2}) / (C_{37:2} + C_{37:3}))$ using the calibration of Müller et al. (1998).

2.4. Total organic carbon (TOC) determination

TOC was measured (following carbonate removal) in a PDZ Europa ANCA-GSL elemental analyzer (1000 °C) at the Stable Isotope Facility of University of California — Davis (USA) within an analytical precision of ±0.09%.

2.5. Age models

The age models were based on the downcore profiles of excess ^{210}Pb determined by gamma spectrometry and confirmed through $^{239+240}Pu$ fallout activities (Sanders et al., 2014). The sediment accumulation rates (SARs) were obtained through the Constant Initial Concentration (CIC) dating method (Appleby and Oldfield, 1992), with $^{210}Pb_{(ex)}$ being fitted

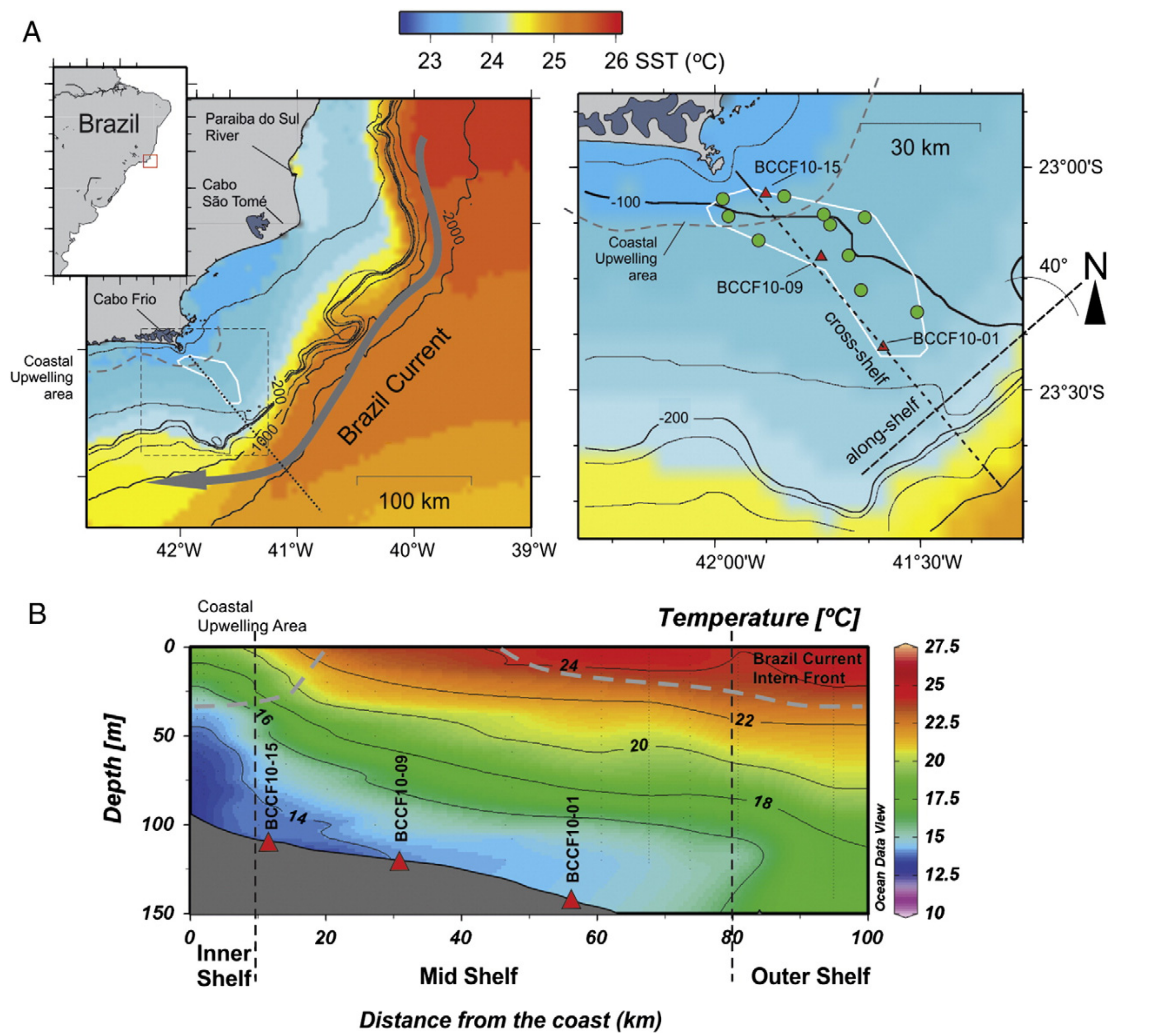

Fig. 1. Cabo Frio continental shelf with the study area indicated with a polygon, the sampling sites highlighted and showing the 10-year mean sea surface temperature (SST) distribution from AVHRR/PFEL-NOAA (A). The 50-year mean temperature distribution along the cross-shelf section obtained from a dataset of ca. 1200 oceanographic stations from the World Ocean Data Center (B). Triangles represent box core samples and circles represent core-top samples.

via the least squares procedure, and the slope of the log-linear curve was used to calculate the SAR.

2.6. Instrumental data

The monthly means of SST from the AVHRR Pathfinder program (Kilpatrick et al., 2001) were obtained from the OceanWatch portal of PFEL/NOAA. This dataset has a spatial resolution of 4.5 km and covers the period from Sep/1981 to Dec/2009, including both day and night passes. Seasonal and annual SST averages were calculated for each core-top sampling location. Monthly SST data from ICOADS (International Comprehensive Ocean–atmosphere Dataset)/ERSST (Enhanced Reconstructed Sea Surface Temperature) Version 3 (Smith et al., 2008) were used to assess oscillations for the 1854–2010 interval. However, due to the coarse 2° resolution of this dataset, a single location in the mid-shelf was taken as being representative of the study area. To assess the annual variation of surface Chlorophyll-a in the area, satellite-derived data were obtained from monthly integrated Sea-viewing Wide Field-of-view Sensor (SeaWiFS) dataset from OceanWatch/NOAA (http://las.pfeg.noaa.gov/oceanWatch) for each sampling location, with a spatial resolution of 0.1°, for the period from 1997 to 2010. Global monthly Upwelling Index (UI) data for the period from 1981 to 2012 were obtained from PFEL/NOAA (http://www.pfeg.noaa.gov/products/las/docs/global_upwell) derived from wind stress data, just for the inshore area, using a coastline orientation of 40° (Bakun, 1973; Schwing et al., 1996).

3. Results and discussion

3.1. Spatial distribution of TOC and alkenones in core-top sediments

TOC contents in surface sediments (core-tops) of the study area ranged from 1.1 to 2.7% (Table 1). They are low compared to those found in eastern boundary upwelling systems, e.g., Peru (Henrichs and Farrington, 1984) and Benguela (Robinson et al., 2002), reflecting lower primary production in the CFUS. However, they contrast with the <1% TOC contents reported for the oligotrophic SEBCM (Mahiques et al., 2004; Rossi-Wongtschowski and Madureira, 2006) and highlight the importance of the upwelling process in the study area. The obtained TOC contents are overall higher than those reported previously by Mahiques et al. (2004) (ca. 1.0–1.8%) and by Yoshinaga et al. (2008) (0.11–1.5%) for the Cabo Frio area. This difference reflects the TOC

Table 1
Sampling locations, TOC contents, concentration of alkenones, sediment accumulation rate, Sea Surface Temperature (SST) derived from alkenone ($U^{K'}_{37}$) and from instrumental data and chlorophyll-a data from the Cabo Frio continental shelf.

Sample #	Lat (°S)	Long (°W)	Water depth (m)	TOC (%)	Chl-a (mg m^{-3})	$U^{K'}_{37}$-SST (°C)	AVHRR-SST (°C)	ΔT (°C)	ΣAlk (μg g^{-1})
CORE-TOPS									
CT-02	23.3252	41.5077	119	1.1	0.27	24.0	23.78	−0.19	1.07
CT-04	23.2764	41.6447	120	2.2	0.29	23.9	23.70	−0.23	1.77
CT-07	23.1121	41.6352	93	1.7	0.34	22.7	22.41	−0.28	0.51
CT-08	23.1982	41.6751	113	2.7	0.34	22.8	22.42	−0.42	1.23
CT-10	23.1284	41.7201	101	1.8	0.36	23.1	22.40	−0.75	1.25
CT-11	23.1054	41.7356	96	1.6	0.36	22.3	22.40	0.12	0.75
CT-12	23.1640	41.8936	121	1.9	0.41	22.7	22.43	−0.29	1.12
CT-13	23.0651	41.8317	82	1.4	0.45	23.3	22.36	−0.98	0.95
CT-14	23.1103	41.9670	113	2.7	0.55	21.9	22.34	0.46	1.08
CT-16	23.0707	41.9810	103	2.4	0.71	22.2	22.0	−0.23	1.23

Sample #	Lat (°S)	Long (°W)	Water depth (m)	[b]TOC (%)	SAR (cm yr^{-1})	[b]$U^{k'}_{37}$-SST (°C)	[b]ERSST (°C)	[b]ΣAlk (μg g^{-1})
[a]*BOX CORES*								
BCCF10-15	23.0586	41.8761	79	1.7 (0.9–2.9)	0.55	22.7 (21.5–23.6)	23.0 (22.5–23.8)	0.53 (0.20–0.89)
BCCF10-09	23.2014	41.7361	117	2.0 (1.0–2.8)	0.17	20.7 (18.9–22.7)	22.8 (22.0–23.7)	6.9 (2.6–14)
BCCF10-01	23.4039	41.5900	128	1.4 (0.7–2.0)	0.10	24.3 (23.6–24.9)	24.0 (23.4–25.2)	0.56 (0.19–0.87)

Chl-a — satellite chlorophyll-a obtained from SeaWiFS; $U^{K'}_{37}$-SST — alkenone-derived sea surface temperature (SST); AVHRR-SST — satellite-derived SST from AVHRR/NOAA; ΔT — difference between instrumental- and alkenone-derived SST; ΣAlk — sum of C_{37} and C_{38} alkenone concentrations; TOC — total organic carbon; SAR — sediment accumulation rate; ERSST — instrumental-derived SST from ICOADS; NA — not applicable.
[a] Downcore distributions are given in the supplementary data (Table 2).
[b] Median values and ranges.

enrichment of the fine-grained sediments of the mud bank, where our sampling stations are located. The inshore and central stations were characterized by higher TOC contents (Table 1).

The concentrations of total alkenones ($C_{37} + C_{38}$: ΣAlk) ranged from 0.51 to 1.8 μg g^{-1}. They also showed higher values in the central area (CT-04 and CT-08) and in the inshore area of CFUS (Table 1, Fig. 2A). When normalized to organic carbon, the alkenone concentrations (9–96 μg g^{-1} C) were higher at the offshore stations (Fig. 2B), consistent with previous results, showing an enhanced contribution of diatom-derived lipids in the organic carbon content of the inshore and central areas (Yoshinaga et al., 2008) as opposed to coccolithophorid-derived alkenones, which appear to be enhanced farther offshore. This finding is in agreement with the typical phytoplankton succession in upwelling systems, which is characterized by diatoms dominating marine productivity in newly upwelled waters, whereas dense coccolithophore communities are found further offshore (e.g. Henderiks et al., 2012). The presence, albeit not dominant, of coccolithophores in upwellings has allowed SST-reconstructions in a number of EBUS (e.g. McGregor et al., 2007; Leduc et al., 2010a; Gutiérrez et al., 2011). In the study area, on-going lipid investigations being done on surface sediments and sediment traps will further define organic matter sources and fluxes, and their spatial/temporal trends.

3.2. Disentangling the $U^{K'}_{37}$-SST signal from core-tops of CFUS

To constrain the application of alkenone-derived SST in CFUS, we present the $U^{K'}_{37}$-SST results for ten core-top (0.5 cm) samples in relation to satellite data in the study area.

The annual mean AVHRR-SSTs (1981–2009) at the core-top locations range from 22.0 to 23.8 °C (Table 1). Monthly means in the study area show that warmer surface waters occur in summer and early autumn (Fig. 3A). After this period SSTs decrease and then rise again in spring. In spring and summer, a conspicuous offshore positive gradient is observed, mainly due to the influence of the BC offshore.

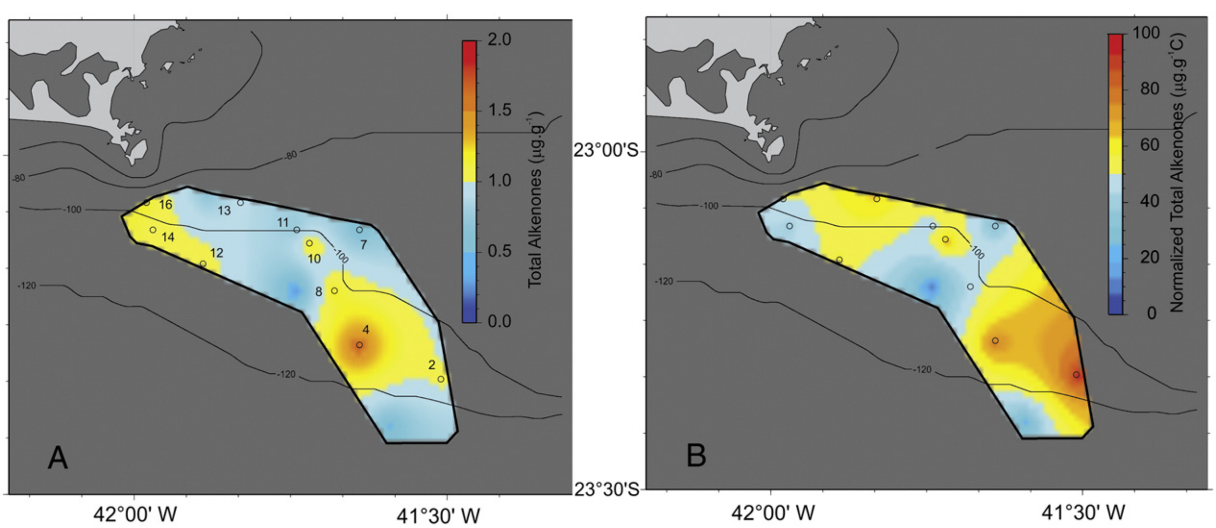

Fig. 2. Spatial variability of the total alkenone concentrations (μg g^{-1}) (A) and carbon-normalized alkenone concentrations (μg g^{-1}C) (B) in core-top sediments from the Cabo Frio continental shelf. The names of the sampling stations are given in map A.

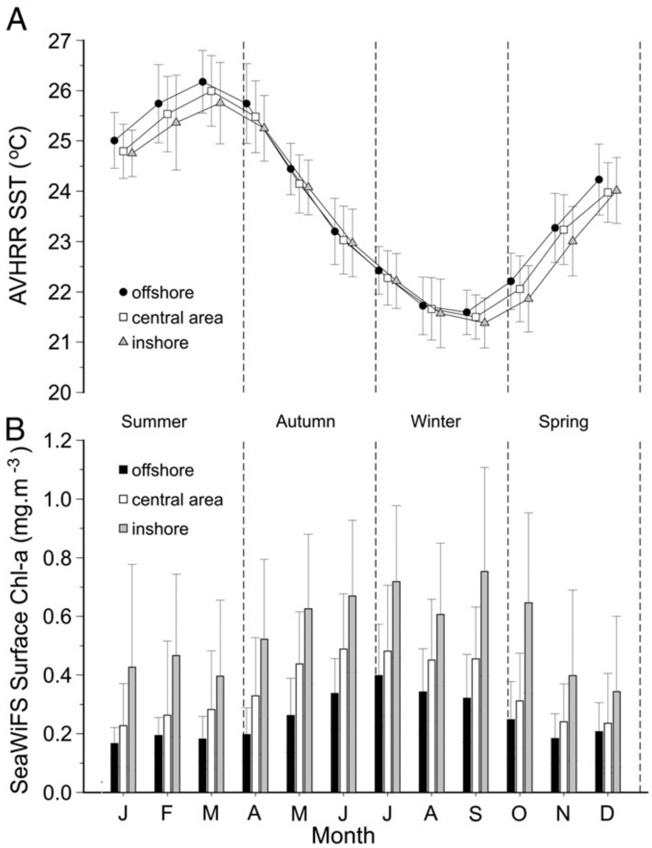

Fig. 3. Satellite-derived SST (AVHRR Pathfinder v.5) (A) and satellite chlorophyll-a (SeaWiFs) (B) monthly mean values (points and bars) and standard errors (lines) from inshore (sampling station #15), central (sampling station #09) and offshore (sampling station #01) areas of the Cabo Frio continental shelf.

The SeaWiFS surface chlorophyll-a (Chl-a) concentrations were inversely related to AVHRR-SSTs, being more abundant during winter/autumn (Fig. 3B) and showing a decreasing trend from inshore (0.71 mg m^{-3}) to offshore (0.27 mg m^{-3}). This spatial pattern of satellite SST and Chl-a is consistent with the influence of coastal upwelling inshore and of warm, oligotrophic BC waters offshore.

The median SST derived from alkenone data ($U^{K'}_{37}$-SST) is 22.8 °C, ranging from 21.9 to 24.0 °C and falling within the range of the annual mean AVHRR-SST (Table 1, Fig. 4A). Similar $U^{K'}_{37}$-SST values were reported by Mahiques et al. (2005) for the last 200 years from a low resolution study of sediment cores in the Cabo Frio coast (ca. 21.5–25.0 °C). Our $U^{K'}_{37}$-SST data in core-tops exhibit an increasing trend from inshore to offshore stations (Fig. 4A), consistent with the influence of cooler upwelling waters closer to the coast and of warmer BC waters offshore. However, the annual mean AVHRR-SSTs do not show this trend (Fig. 4B), being higher than $U^{K'}_{37}$-SST in the inshore and the central areas of CFUS. Taking into account that satellite-derived SST data show a relevant seasonal pattern (Fig. 3), we explored possible seasonal responses of the $U^{K'}_{37}$-SST that would account for the discrepancies observed between $U^{K'}_{37}$-SST and mean annual satellite-SST. We found that $U^{K'}_{37}$-SSTs at inshore and central stations better reflect winter/spring SST means than annual means (Fig. 4A–B–C, see also Fig. 6 in the supplementary data), likely recording local conditions such as coastal upwelling events. However, the warmer $U^{K'}_{37}$-SST values offshore reconstruct the annual mean SST of the dominant BC waters (or the thermal front). Thus, the $U^{K'}_{37}$-SSTs in the study area better fit with a composite spring/winter (inshore and central areas) and annual (offshore) satellite-SSTs (Fig. 4D), showing a significant correlation (0.72, $p < 0.05$, Spearman). Our findings highlight the need for caution when paleoenvironmental conditions are reconstructed from a single core in dynamic and complex continental shelf systems like the Cabo Frio setting.

The differences between instrumental and proxy data ($\Delta T = AVHRR\text{-}SST - U^{K'}_{37}\text{-}SST$) are <1 °C for the core-top samples (Table 1), smaller than previously reported by Benthien and Müller (2000) in a SW Atlantic study. The $U^{K'}_{37}$-SST values reported by these authors were considered to be in agreement with instrumental data for areas close to CFUS (the western tropical Atlantic, Brazil Current region and South Atlantic Tropical Gyre north of 32°S). Overall, our study on core-tops from the CFUS shows that the $U^{K'}_{37}$-SST proxy and the global calibration of Müller et al. (1998) yield reliable SST data in the study area, provided that the core location is taken into account when interpreting the data.

3.3. SST oscillations over the century

Estimated sedimentation rates (SAR) are different for the three sediment cores we studied (0.10 to 0.55 cm yr^{-1}, Table 1). Thus, core BCCF10-15 in the inshore area recovered the last 36 years (time resolution of ca 2 years), whereas core BCCF10-09 (central area) and core BCCF10-01 (offshore area) recovered the last 112 and 164 years, with a time resolution of ca. 6 and 9 years, respectively. Because age models based on ^{210}Pb can be applied with confidence up to 130 years (Binford, 1990) cal. ages from 1846 to 1883 in the offshore core were estimated based on linear regressions.

Differences between mean ERSST and $U^{K'}_{37}$-SST values are ca. 0.3 °C for the inshore and offshore cores, but higher (2.1 °C) in the central core (Table 1), where the lowest $U^{K'}_{37}$-SSTs were observed (see discussion below). This discrepancy can be attributed to the low spatial resolution (2° × 2°) of the ERSST data, which may not properly capture in detail SST variations on the shelf, especially those likely related to upwelling, where gridded data sets are likely to smooth out the cooler upwelled waters.

The $U^{K'}_{37}$-SST values showed different temperature ranges for each area of CFUS. Consistent with the core-top data, higher values are found in the offshore core (23.6–24.9 °C). However, SST values were lower in the central area (18.9–22.7 °C) than in the inshore area (21.5–23.6 °C) (Table 1, Fig. 5).

In the inshore area (core BCCF10-15), $U^{K'}_{37}$-SSTs show a significant short-term variability superimposed on a general trend of cooling in the last ca. 36 years (Fig. 5). Here, SST appears to be controlled by coastal upwelling events inasmuch as the $U^{K'}_{37}$-SST and PFEL/NOAA global upwelling index show roughly opposite trends (Fig. 5). However, admixture with warm Coastal Waters may have also modulated the SST values. Both $U^{K'}_{37}$-SST and the global upwelling index likely suggest intensification of coastal upwelling over the last 30 years.

On the central area (core BCCF10-09), $U^{K'}_{37}$-SSTs show lowest values (18.9–22.7 °C, Fig. 5) suggesting that this location preferentially records the influence of the upwelled SACW. Highest TOC values and alkenone concentrations (Table 1) are also consistent with upwelling-driven productivity signals, and associated proxies, being preferentially recorded in the central sediments. These signals derive from phytoplankton productivity developing in the overlying surface waters and/or in surface waters from the inshore area, where upwelling and productivity are enhanced (higher Chl-a concentrations, Fig. 3B). Both upwelling plumes and particle advection favor such a cross-shelf transport. In addition, oceanographic features of CFUS, such as the fluctuation of SACW and the displacement of the thermal front of BC, seem to enhance lateral transport from inshore to adjacent offshore areas. The $U^{K'}_{37}$-SST record in core BCCF10-09 also shows a gradual cooling trend (Fig. 5), suggesting increasing influence of the SACW, and thus upwelling strengthening, during the last century.

In the offshore area (core BCCF10-01), the $U^{K'}_{37}$-SST data reflect an overall smooth cooling from 1840 to 1955 and then a slight warming until the present. Offshore, SST variability is related to oscillations in the position of the thermal front of the BC. When the thermal front is

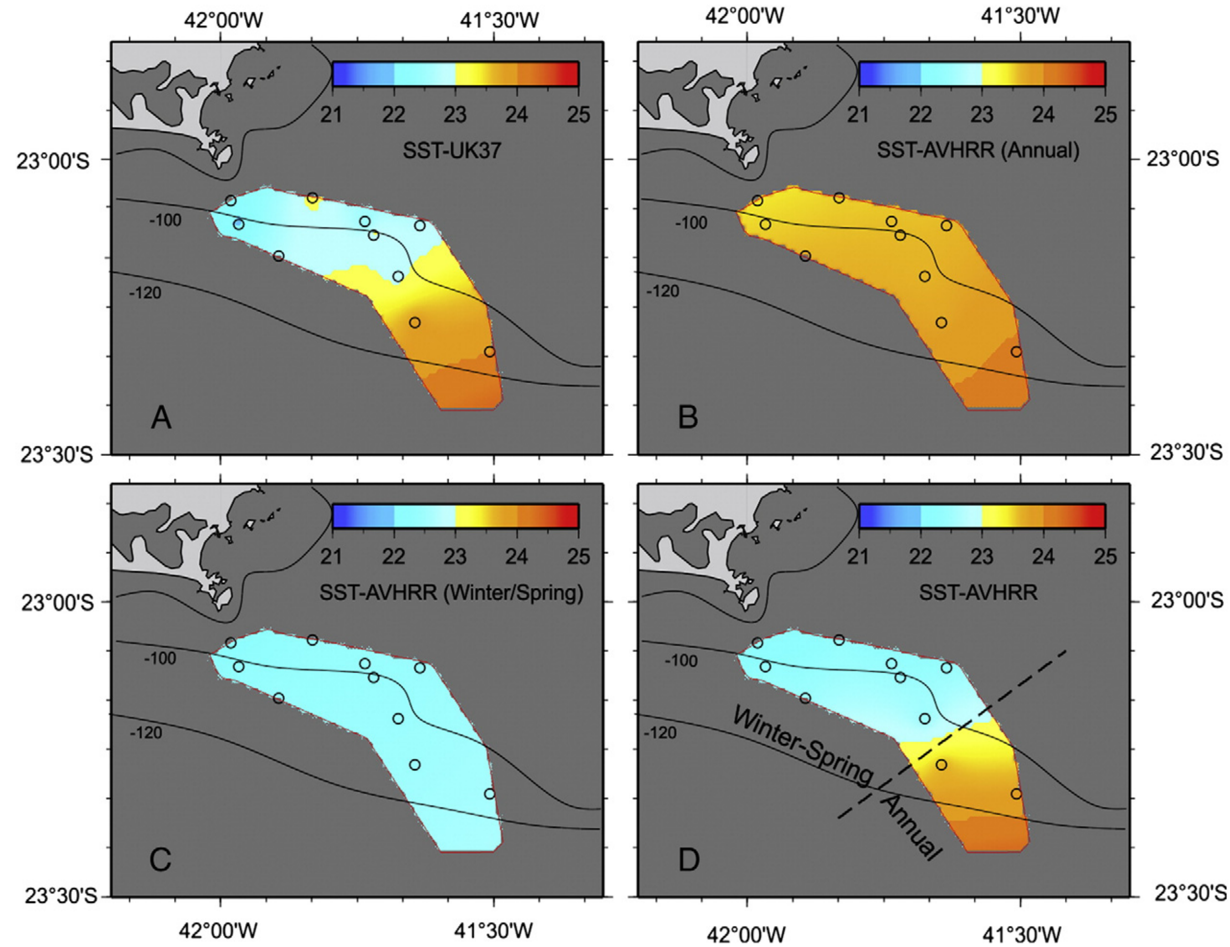

Fig. 4. $U^{K'}_{37}$-SST in core-top samples (A), annual mean AVHRR-SST (B), winter/spring mean AVHRR-SST (C) and the composition of the winter/spring mean AVHRR-SST at inshore and central areas and the annual mean AVHRR-SST at offshore area (D) on the Cabo Frio continental shelf.

closer to the coast, SSTs increase, whereas when it is more distant, other mechanisms in the shelf region are enhanced, including SACW shoaling and coastal upwelling, resulting in lower SSTs. The adjustment of the BC registered in the offshore core of the CFUS since ~1950 can be associated with the intensification of zonal winds across the tropical Atlantic due to climate change, resulting in the piling up of warmer BC waters closer to

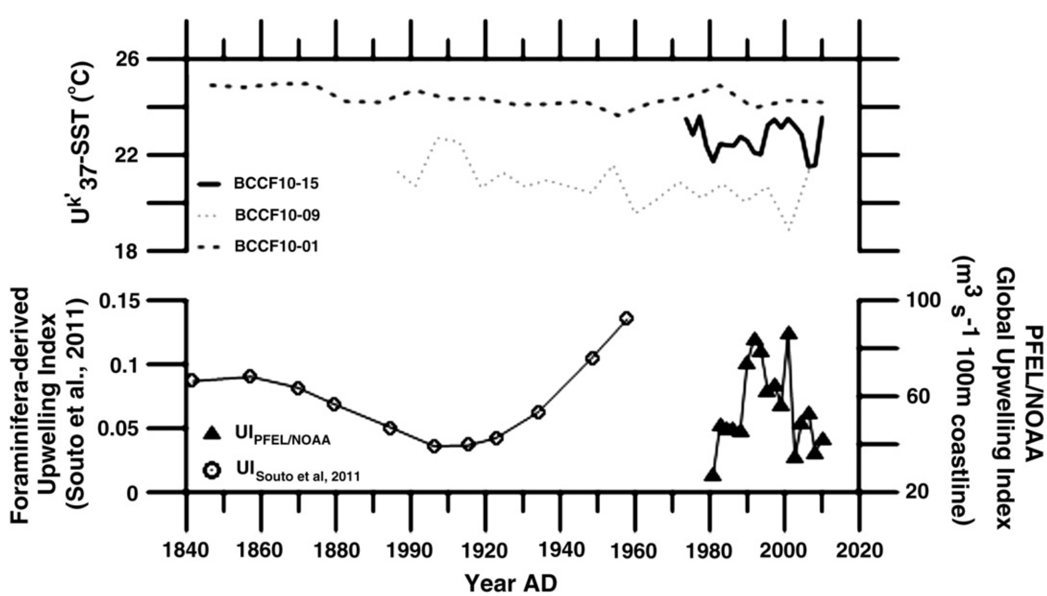

Fig. 5. Temporal oscillations of alkenone-derived SST ($U^{K'}_{37}$-SST) obtained for the inshore core (BCCF10-15), the central core (BCCF10-09) and the offshore core (BCCF10-01) and temporal oscillations of the PFEL/NOAA global upwelling index and the foraminifera-derived upwelling index estimated from the Gb/Gr ratio (*Globigerina bulloides* and *Globigerina ruber* planktonic foraminifera ratio) by Souto et al. (2011) on the Cabo Frio continental shelf.

the coast. Increasing zonal winds, due to the repositioning of the Intertropical Convergence Zone (ITCZ), as part of the whole South Atlantic atmosphere–ocean circulation system, can increase the momentum transfer to the geostrophic currents, such as the BC, which is reflected immediately in its flow, through instabilities (Carton and Huang, 1994; Perez et al., 2011; Doi et al., 2012).

Souto et al. (2011), using the foraminifera-derived upwelling index, (Fig. 5) and Mahiques et al. (2005), using SSTs reconstructed from alkenones, similarly reported intensification of the Cabo Frio coastal upwelling and associated it with regional atmospheric factors. Souto et al. (2011) related the intensification of the Cabo Frio upwelling from 1500 to 1830 AD to a southward displacement of the ITCZ, caused by a cooling of the North Atlantic during the Little Ice Age (1400–1800), and that, associated with the intensification and southern positioning of the SAH, could have intensified the NE winds over Cabo Frio and consequently induced upwelling. Intriguingly, recent intensification of coastal upwelling has also been reported for a number of eastern boundary systems, such as on the northwestern African margin (McGregor et al., 2007), the southern Benguela Upwelling System (Leduc et al., 2010a) and the Peru upwelling system (Gutiérrez et al., 2011).

4. Summary and conclusions

1. Investigation of alkenones in core-top sediments from the CFUS and comparison with instrumental data allowed for constraining the application of the $U^{K'}_{37}$ proxy for SST reconstructions in the study area. The inshore and central sediments are found to record mainly coastal upwelling, with the central area appearing as preferentially capturing the upwelling-related SST signal. SST in the offshore area is mainly controlled by the position of the thermal front of the Brazil Current.
2. Observed cross-shelf spatial heterogeneities in SST call for caution when paleoenvironmental conditions in complex and dynamic continental shelf systems are reconstructed from only a single core. They also highlight the need for complementary investigations in modern settings and comparisons with instrumental data.
3. During the last century a conspicuous SST decline was observed in the inshore and central areas, suggesting intensification of coastal upwelling and of subsurface intrusion of SACW. The intensification of upwelling mechanisms can be related to the southern displacement of the ITCZ and SAH, promoting enhanced NE winds involved with driving upwelling. In parallel, the cross-shore SST gradient increased, despite the smooth cooling observed at the offshore area. The slight warming of offshore waters over the last ca. 60 years can be related to the adjustment of the BC since ~1950, which is possibly associated with the intensification of zonal winds in the South Atlantic due to climate change.

Supplementary data to this article can be found online at http://dx.doi.org/10.1016/j.palaeo.2014.01.020.

Acknowledgments

This work was financially supported through the Ressurgência Project by the Geochemistry Network of PETROBRAS/CENPES, by the National Petroleum Agency (ANP) of Brazil (Grant 0050.004388.08.9) and by LOCEAN-IPSL (CNRS/IRD/UPMC/MNHN). We thank the Projeto PRIMO (CNPq-590172/2011-5) for general support, the Ressurgência Project team for the assistance in sampling and sample preparation, and V. Klein and F. Kaczmar at LOCEAN for the analytical assistance. We are grateful to the two anonymous reviewers for their constructive comments that greatly contributed in improving the manuscript.

References

Aidar, E., Gaeta, S.A., Gianesella-Galvão, S.M.F., Kutner, M.B.B., Teixeira, C., 1993. Ecossistema costeiro subtropical: nutrientes dissolvidos, fitoplâncton e clorofila-a e suas relações com as condições oceanográficas na região de Ubatuba (SP). Publ. Espec. Inst. Oceanogr. Sao Paulo 10, 9–43.

Appleby, P.G., Oldfield, F., 1992. Application of lead-210 to sedimentation studies. In: Ivanovich, M., Harman, R.S. (Eds.), Uranium-Series Disequilibrium: Application to Earth, Marine, and Environmental Sciences. Clarendon Press, Oxford.

Bakun, A., 1973. Coastal upwelling indices, west coast of North America, 1946–71. NOAA Technical Report NMFS SSRF-671US Dept. of Commerce (103 pp.).

Belem, A.L., Castelao, R.M., Albuquerque, A.L., 2013. Controls of subsurface temperature variability in a western boundary upwelling system. Geophys. Res. Lett. 40, 1362–1366.

Benthien, A., Müller, P.J., 2000. Anomalously low alkenone temperatures caused by lateral particle and sediment transport in the Malvinas Current region, western Argentine Basin. Deep-Sea Res. I 47, 2369–2393.

Binford, M.W., 1990. Calculation and uncertainty analysis of 210Pb dates for PIRLA project lake sediment cores. J. Paleolimnol. 3 (3), 253–267.

Campos, E.J.D., Velhote, D., da Silveira, I.C.A., 2000. Shelf break upwelling driven by Brazil Current cyclonic meanders. Geophys. Res. Lett. 27 (6), 751–754.

Carton, J.A., Huang, B., 1994. Warm events in the tropical Atlantic. J. Phys. Oceanogr. 24, 888–903.

Carvalho, L.M., Jones, C., Liebmann, B., 2004. The South Atlantic convergence zone: Intensity, form, persistence, and relationships with intraseasonal to interannual activity and extreme rainfall. J. Clim. 17 (1), 88–108.

Castelao, R.M., Barth, J.A., 2006. Upwelling around Cabo Frio, Brazil: the importance of wind stress curl. Geophys. Res. Lett. 33, 1–4.

Castro, B.M.F., Miranda, L.B., 1998. Physical oceanography of the western Atlantic continental shelf located between 4°N and 34°S. In: Robinson, A.R., Brink, K.H. (Eds.), The Sea, 11. John Wiley & Sons, New York, pp. 209–251.

Castro, B.M.F., Miranda, L.B., Miyao, S., 1987. Condições hidrográficas na plataforma continental ao largo de Ubatuba: variações sazonais e em média escala. Bol. Inst. Oceanogr. 35 (2), 135–151.

Chaves, R.R., Nobre, P., 2004. Interactions between sea surface temperature over the South Atlantic Ocean and the South Atlantic Convergence Zone. Geophys. Res. Lett. 31 (3), L03204. http://dx.doi.org/10.1029/2003GL018647.

Cruz, A.P., Barbosa, C.F., Ayres-Neto, A., Albuquerque, A.L.S., 2013. Physical and geochemical properties of centennial marine sediments of the continental shelf of southeast Brazil. Geochim. Bras. 27 (1), 1–12.

Dias, G., Palma, J.J.C., et al., 1982. Matéria orgânica no quaternário da margem continental entre Rio de Janeiro e Guarapari. Projeto “Ressurgência”, LAGEMAR IG/UFRJ — PETROBRAS, Relatório final. Rio de Janeiro. Brasil (32 pp.).

Doi, T., Vecchi, G.A., Rosati, A.J., Delworth, T.L., 2012. Biases in the Atlantic ITCZ in seasonal-interannual variations for a coarse- and a high-resolution coupled climate model. J. Clim. 25, 5494–5511.

Estrada, M., 1980. Phytoplankton biomass and production in the upwelling region of NW Africa. Relationships with hidrographic parameters. Mar. Biol. 60, 63–71.

Franchito, S.H., Oda, T.O., Rao, V.B., Kayano, M.T., 2008. Interaction between coastal upwelling and local winds at Cabo Frio, Brazil: an observational study. J. Appl. Meteorol. Climatol. 47 (6), 1590–1598.

Gonzalez-Rodriguez, E., Valentin, J.L., André, D.L., Jacob, S.A., 1992. Upwelling and downwelling at Cabo Frio (Brazil): comparison of biomass and primary production responses. J. Plankton Res. 14 (2), 289–306.

Gutiérrez, D., Bouloubassi, I., Sifeddine, A., Purca, S., Goubanova, K., Graco, M., Field, D., Méjanelle, L., Velazco, F., Lorre, A., Salvatteci, R., Quispe, D., Vargas, G., Dewitte, B., Ortlieb, L., 2011. Coastal cooling and increased productivity in the main upwelling zone off Peru since the mid-twentieth century. Geophys. Res. Lett. 38, L07603. http://dx.doi.org/10.1029/2010GL046324.

Henderiks, J., Winter, A., Elbrächter, M., Feistel, R., van der Plas, A., Nausch, G., Barlow, R., 2012. Environmental controls on *Emiliania huxleyi* morphotypes in the Benguela coastal upwelling system (SE Atlantic). Mar. Ecol. Prog. Ser. 448, 51–66.

Henrichs, S.M., Farrington, J.W., 1984. Peru upwelling region sediments near 15°S. Remineralization and accumulation of organic matter. Limnol. Oceanogr. 29 (1), 1–19.

Herbert, T.D., 2003. Alkenone paleotemperature determinations. In: Holland, H.D., Turekian, K.K. (Eds.), Treatise on Geochemistry. , 6. Elsevier, pp. 391–432.

Jaeschke, A., Rühlemann, C., Arz, H., Heil, G., Lohmann, G., 2007. Coupling of millennial-scale changes in sea surface temperature and precipitation off northeastern Brazil with high-latitude climate shifts during the last glacial period. Paleoceanography 22, PA4206. http://dx.doi.org/10.1029/2006PA001391.

Kilpatrick, K.A., Podesta, G.P., Evans, R., 2001. Overview of the NOAA/NASA Advanced Very High Resolution Radiometer Pathfinder algorithm for sea surface temperature and associated matchup database. J. Geophys. Res. Oceans 106 (C5), 9179–9197.

Kim, J.-H., Schneider, R.R., Müller, P.J., Wefer, G., 2002. Interhemispheric comparison of deglacial sea-surface temperature patterns in Atlantic eastern boundary currents. Earth Planet. Sci. Lett. 194, 383–393.

Kim, J.-H., Schneider, R.R., Mulitza, S., Müller, P.J., 2003. Reconstruction of SE trade wind intensity based on sea-surface temperature gradients in the SE Atlantic over the last 25 kyr. Geophys. Res. Lett. 30, 2144. http://dx.doi.org/10.1029/2003GL017557.

Kim, J.-H., Schouten, S., Hopmans, E.C., Donner, B., Damsté, J.S.S., 2008. Global sediment core-top calibration of the TEX86 paleothermometer in the ocean. Geochim. Cosmochim. Acta 72, 1154–1173.

Leduc, G., Schneider, R., Kim, J.-H., Lohmann, J., 2010a. Holocene and Eemian sea surface temperature trends as revealed by alkenone and Mg/Ca paleothermometry. Quat. Sci. Rev. 29, 989–1004. http://dx.doi.org/10.1016/j.quascirev.2010.01.004.

Leduc, G., Herbert, C.T., Blanz, T., Martinez, P., Schneider, R., 2010b. Contrasting evolution of sea surface temperature in the Benguela upwelling system under natural and anthropogenic climate forcings. Geophys. Res. Lett. 37, L20705. http://dx.doi.org/10.1029/2010GL044353.

Liebmann, B., Marengo, J., 2001. Interannual variability of the rainy season and rainfall in the Brazilian Amazon Basin. J. Clim. 14 (22), 4308–4318.

Lorenzzetti, J.A., Gaeta, S.A., 1996. The Cape Frio Upwelling effect over the South Brazil Bight northern sector shelf waters: a study using AVHRR images. Int. Arch. Photogramm. Remote. Sens. XXXI (Part B7).

Mahiques, M.M., Tessler, M.G., Ciotti, A.M., Silveira, I.C.A., Sousa, S.H.M., Figueira, R.C.L., Tassinari, C.C.G., Furtado, V.V., Passos, R.F., 2004. Hydrodynamically driven patterns of recent sedimentation in the shelf and upper slope off Southeast Brazil. Cont. Shelf Res. 24, 1685–1697.

Mahiques, M.M., Bícego, M.C., Silveira, I.C.A., Souza, S.H.M., Lourenço, R., Fukumoto, M.M., 2005. Modern sedimentation in the Cabo Frio upwelling system, Southeastern Brazilian shelf. An. Acad. Bras. Cienc. 77 (3), 535–548.

Marone, E., Knoppers, B.A., Souza, W.F.L., Silveira, I.C.A., Godoi, S.S., 2010. The Brazil Current: physical–biogeochemical domains. In: Liu, K.-K., Atkinson, L., Quiñones, R., Talaue-Macmanus, L. (Eds.), Carbon and Nutrient Fluxes in Continental Margins: A Global Synthesis. Springer, Berlin, pp. 153–170.

McGregor, H.V., Dima, M., Fischer, H.W., Mulitza, S., 2007. Rapid 20th century increase in coastal upwelling off northwest Africa. Science 315, 637–639.

Moreira da Silva, P.C., 1971. Upwelling and its biological effects in southern Brazil. In: Costlow, J.D. (Ed.), Fertility of the Sea. Gordon & Breach, New York, pp. 469–474.

Moreira da Silva, P.C., 1973. A ressurgência de Cabo Frio (I). Bol. Inst. Pesqui. Mar. 78, 60.

Müller, P.J., Kirst, G., Ruhland, G., Von Storch, I., Rosell-Melé, A., 1998. Calibration of the alkenone paleotemperature index UK′37 based on core-tops from the eastern South Atlantic and the global ocean (60°N–60°S). Geochim. Cosmochim. Acta 62 (10), 1757–1772.

Perez, R.C., Garzoli, S.L., Meinen, C.S., Matano, R.P., 2011. Geostrophic velocity measurement techniques for the meridional overturning circulation and meridional heat transport in the South Atlantic. J. Atmos. Ocean. Technol. 28, 1504–1521.

Robertson, A.W., Mechoso, C.R., 2000. Interannual and interdecadal variability of the South Atlantic Convergence Zone. Mon. Weather Rev. 128, 2947–2957.

Robinson, R.S., Meyers, P.A., Murray, R.W., 2002. Geochemical evidence for variations in delivery and deposition of sediment in Pleistocene light–dark color cycles under the Benguela Current Upwelling System. Mar. Geol. 180, 249–270.

Rodrigues, R.R., Lorenzzetti, J.A., 2001. A numerical study of the effects of bottom topography and coastline geometry on the Southeast Brazilian coastal upwelling. Cont. Shelf Res. 21, 371–394.

Rosell-Melé, A., Prahl, F.G., 2013. Seasonality of UK′37 temperature estimates as inferred from sediment trap data. Quat. Sci. Rev. 72, 128–136.

Rossi-Wongtschowski, C.L., Madureira, L.A.S., 2006. O ambiente oceanográfico da plataforma continental e do talude da região sudeste-sul do Brasil. EdUSP, São Paulo.

Sachs, J.P., Anderson, R.F., 2003. Fidelity of alkenone paleotemperature reconstructions in southern Cape Basin sediment drifts. Paleoceanography 16 (4), 1082. http://dx.doi.org/10.1029/2002PA000862.

Sachs, J.P., Pahnke, K., Smittenberg, R., Zhang, Z., 2007. Biomarker indicators of past climate. In: Elias, S.A. (Ed.), Encyclopedia of Quaternary Science. Elsevier, Amsterdam.

Sanders, C.J., Caldeira, P.P., Smoak, J.M., Ketterer, M.E., Belem, A.L., Mendoza, U.M., Cordeiro, L.G., Silva-Filho, E.V., Patchineelam, S.R., Albuquerque, A.L.S., 2014. Recent organic carbon accumulation (~100 years) along the Cabo Frio, Upwelling Region, Brazil. Cont. Shelf Res 75, 68–75. http://dx.doi.org/10.1016/j.csr.2013.10.009.

Schwing, F.B., O'Farrel, M., Steger, J.M., Baltz, K., 1996. Coastal upwelling indices, west coast of North America, 1946–95. NOAA Technical Memorandum NOAA-TM-NMFS-SWFSC-231US Dept. of Commerce (45 pp.).

Silveira, I.C.A., Lima, J.A.M., Schmidt, A.C.K., Ceccopieri, W., Sartori, A., Fransisco, C.P.F., Fontes, R.F.C., 2008. Is the meander growth in the Brazil Current system off Southeast Brazil due to baroclinic instability? Dyn. Atmos. Oceans 45, 187–207.

Smith, T.M., Reynolds, R.W., Peterson, T.C., Lawrimore, J., 2008. Improvements to NOAA's historical merged land-ocean surface temperature analysis (1880–2006). J. Clim. 21, 2283–2296.

Souto, D.D., Lessa, D.V.O., Albuquerque, A.L.S., Sifeddine, A., Turcq, B., Barbosa, C.F., 2011. Marine sediments from southeastern Brazilian continental shelf: a 1200 year record of upwelling productivity. Palaeogeogr. Palaeoclimatol. Palaeoecol. 299, 49–55.

Strickland, J.D.H., Eppley, R.W., Mendiola, B.R., 1969. Phytoplankton populations, nutrients and photosynthesis in the Peruvian coastal waters. Bol. Inst. Mar Peru 2 (1), 37–45.

Valentin, J.L., 1984. Analyse des paramètres hydrobiologiques dans la remontée de Cabo Frio (Brésil). Mar. Biol. 82, 259–276.

Valentin, J.L., Coutinho, R., 1990. Modelling maximum chlorophyll in the Cabo Frio (Brazil) upwelling: a preliminary approach. Ecol. Model. 52, 103–113.

Valentin, J.L., Kempf, M., 1977. Some characteristics of the Cabo Frio upwelling. Coast. Upwelling Ecosyst. Anal. Newsl. 6 (2), 18–19.

Valentin, J.L., André, D.L., Jacob, S.A., 1987. Hydrology in the Cabo Frio (Brazil) upwelling: two-dimensional structure and variability during a wind cycle. Cont. Shelf Res. 7 (1), 77–88.

Yoshinaga, M.Y, Sumida, P.G., Wakeham, S.G., 2008. Lipid biomarkers in surface sediments from an unusual coastal upwelling area from the SW Atlantic Ocean. Org. Geochem. 39, 1385–1399.

Zhou, J., Lau, K.M., 1998. Does a monsoon climate exist over South America? J. Clim. 11 (5), 1020–1040.